ANEXO 1

Patarroyo ME, **Alba MP**, Curtidor H. Biological and structural characteristics of the binding peptides from the sporozoite proteins essential for cell traversal (SPECT)-1 and -2. Peptides. 2011. 32:154-60

Peptides xxx (2010) xxx–xxx

Contents lists available at ScienceDirect

Peptides

journal homepage: www.elsevier.com/locate/peptides

Short communication

Biological and structural characteristics of the binding peptides from the sporozoite proteins essential for cell traversal (SPECT)-1 and -2

Manuel E. Patarroyo[a,c,*], Martha P. Alba[a,b], Hernando Curtidor[a,b]

[a] Fundación Instituto de Inmunología de Colombia FIDIC, Bogotá, Colombia
[b] Universidad del Rosario, Bogotá, Colombia
[c] Universidad Nacional de Colombia, Bogotá, Colombia

ARTICLE INFO

Article history:
Received 9 August 2010
Received in revised form
29 September 2010
Accepted 29 September 2010
Available online xxx

Keywords:
Antimalarial vaccine
High-activity binding peptides (HABPs)
Plasmodium falciparum
SPECT-1
SPECT-2
^{1}H NMR

ABSTRACT

The sporozoite microneme proteins essential for cell traversal, SPECT-1 and SPECT-2, are considered attractive pre-erythrocytic immune targets due to the key role they play in crossing of the malaria parasite across the dermis and the liver sinusoidal wall, prior to invasion of hepatocytes. In this study, the sequences of SPECT-1 and SPECT-2 were mapped using 20 mer-long synthetic peptides to identify high-activity binding peptides (HABPs) to HeLa cells. 17 HABPs with enzyme sensitive bindings to HeLa cells were identified: 3 predominantly α-helical in SPECT-1, and 10 α-helical and 4 β-turns/random coils in SPECT-2. Immunofluorescence assays (IFA) with antibodies raised in rabbits against chemically synthesized B-cell epitopes suggests the presence of these two proteins in the micronemes and in sporozoite membrane. ^{1}H NMR studies showed that HABPs located in the membrane-attack complex/perforin (MACPF) domain of SPECT-2 share high similarity with the 3D structure of C8α. Altogether, the results highlight the potential of including HABPs from SPECT-1 and SPECT-2 as components of a fully effective multistage, multiepitopic, minimal subunit-based synthetic vaccine against *Plasmodium falciparum* malaria.

1. Introduction

During the development of the most lethal form of human malaria, a disease causing around 500 million cases and more than 3 million deaths worldwide each year [22], different forms of the *Plasmodium falciparum* parasite recognize and invades at least two types of human cells: liver cells and red blood cells (RBCs) [5,12] through a process that involves using a wide variety of parasite proteins [17,20].

The pathogen's life cycle begins when an infected *Anopheles* mosquito injects 100–1000 sporozoites (larvae like structures, as seen in Fig. 1A) into the skin of the human host during a blood meal. These sporozoites have to go across the dermis to reach blood vessels, travel to the liver via the bloodstream and cross the sinusoidal wall by passing through the Kupffer cells (the macrophages of the liver) to finally invade hepatocytes, in a process mediated by specific interactions between host–cell receptors and parasite proteins [5,12,27]. To date, the most studied pre-erythrocytic invasins are the circumsporozoite protein (CSP) [12,27] and the thrombospondin-related anonymous protein (TRAP) [1] both involved in traversal of mammalian cells and sporozoite invasion of hepatocytes.

Two recently described parasite proteins are essential for sporozoite traversal of the dermis and Kupffer cells, namely SPECT-1 and SPECT-2 [8,9]. The 28 kDa SPECT-1 and 95 kDa SPECT-2 (also known as *Plasmodium* perforin-like protein-1 or PPLP-1) are stored in the micronemes and later on translocated to the sporozoite's membrane during the infection of the vertebrate host. Targeted disruption of both genes has been shown to affect sporozoite infectivity *in vivo*, and completely abolish traversal of HeLa cells *in vitro*, suggesting that SPECT molecules are important for the parasite's ability to cross cell barriers, particularly for the progression of the sporozoite from the dermis to the hepatocyte, as elegantly shown by Amino et al. [2]. Interestingly, no effect has been observed on the gliding motility, crossing of blood and lymphatic vessels of the dermis or hepatocyte infection capacity of *spect-1* (−) and *spect-2* (−) knock-down parasites *in vivo*, while depletion of Kupffer cells in mice restores parasite infectivity to hepatocytes back to normal levels, suggesting that they could be arrested by phagocytic cells in the dermis [2] and Kupffer cells of the liver [8,9].

Although the mechanisms by which SPECT-1 and SPECT-2 participate in cell traversal of sporozoites is still unknown, the presence of a membrane-attack complex/perforin (MACPF) domain in SPECT-2 [8,11] has suggested a pore formation mechanism, similar to that of the mammalian C8α complement cascade MACPF protein

* Corresponding author at: Fundación Instituto de Inmunología de Colombia, Carrera 50 No 26-20, Bogotá, Colombia. Tel.: +57 1 4815219; fax: +57 1 4815269.
E-mail address: mepatarr@mail.com (M.E. Patarroyo).

0196-9781/$ – see front matter © 2010 Published by Elsevier Inc.
doi:10.1016/j.peptides.2010.09.026

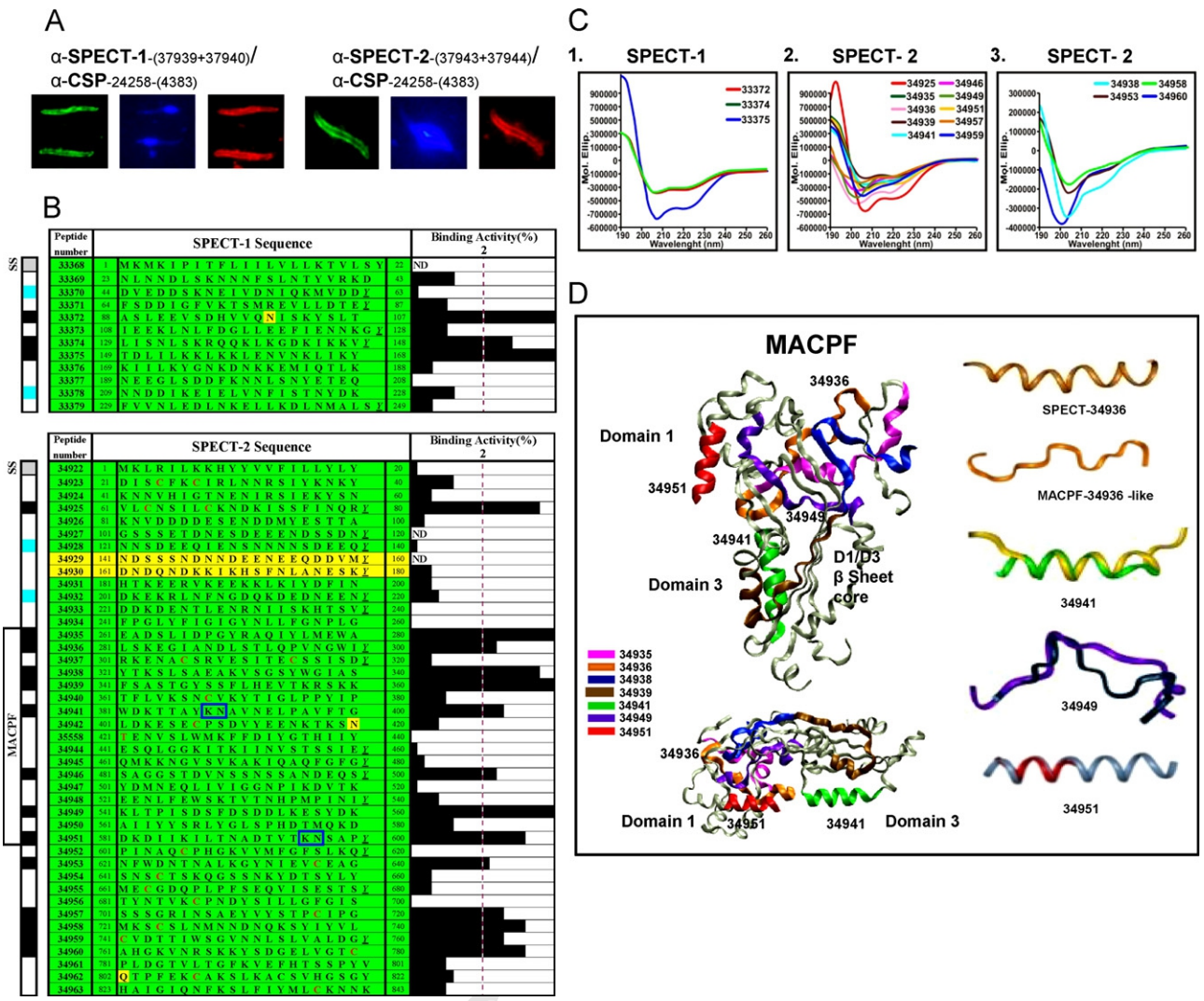

Fig. 1. (A) Immunofluorescence assays with rabbit anti-SPECT-1 (peptides A mixture) and anti-SPECT-2 (peptides B mixture) antisera, showing a peripheral and punctuate-like immunofluorescence pattern in sporozoites, characteristic of membrane and micronemal sporozoite proteins presence (green fluorescence). In co-localization studies anti Pf. CSP *Aotus* sera show the same membranal and micronemal pattern (red fluorescence). In the central picture, bright blue colour corresponds to DAPI staining of the sporozoite's nuclei. Pre-immune sera showed no reactivity (data not shown). (B) Binding profiles of SPECT-1 and SPECT-2 synthetic peptides (numbered according to our institute serial number) to HeLa cells. Binding activities are represented by the length of the horizontal black bars. Schematic representations of SPECT-1 and SPECT-2 are shown to the left of each binding profile, showing the localization of the membrane-attack complex/perforin (MACPF)-related domain, signal sequences (SS; gray boxes), HABPs (black boxes) and polymeric peptides inoculated in rabbits to obtain antisera (pale blue boxes). In the aminoacids sequences, cysteines (red), sulfate-binding KN sequences (boxed), conserved sequences (green), and variable regions (yellow) are indicated. ND = Not determined. In the SPECT-2 peptide 35558, a C residue was replaced by T (shown in red). (C). Circular dichroism spectra of SPECT-1 (1) and SPECT-2 HABPs in 30% TFE. SPECT-2 spectra were grouped according to their structural features: (2) alpha helix and (3) random coil. (D). Frontal and lateral view of C8α MACPF 3D structure determined by X-ray crystallography (PDB code 2QQH), showing the theoretical localization of the SPECT-2 HABPs 34935, 34936, 34938, 34939, 34941, 34949 and 34951 in the C8α MACPF molecule. HABPs are colored according to the color code shown below. It is also shown the superimposition of the 3D structures of HABPs (determined by ^{1}H NMR) and the C8α MACPF domain, colored according to the color code shown below. (For interpretation of the references to color in this figure legend, the reader is referred to the web version of the article.)

family, structurally and functionally very similar to the family of pore-forming toxins, also named cholesterol-dependent cytolysins or CDCs.

In the development of a multistage, multiantigenic, minimal subunit-based, chemically synthesized antimalarial vaccine, we have finely mapped a large number of parasite proteins in order to identify their high-activity binding peptides (HABPs) to different host cells targeted by *P. falciparum* [5,13,17,20], and have used these peptides to design potential components of a fully effective antimalarial vaccine [14]. Based on the relevance of SPECT-1 and SPECT-2 for the cell-traversal activity of sporozoites *in vivo* and *in vitro*, 20 mer-long non-overlapping synthetic peptides spanning the entire sequences of these proteins were tested using the highly robust, sensitive and specific methodology previously described [20], to identify which sequences specifically interact with HeLa cells. Structural characteristics relevant for performing appropriate modifications to render these HABPs into highly immunogenic protection-inducing peptides were determined by ^{1}H NMR, and the so obtained structures were superimposed on the 3D structure of the C8α MACPF domain, displaying a high degree of similarity at the atomic level.

2. Materials and methods

2.1. Peptide synthesis and radiolabeling

Fifty four non-overlapping peptides covering the amino acid sequences of the *P. falciparum* 3D7 SPECT-1 (MAL13P1.212) and SPECT-2 (PFD0430c) proteins were synthesized using t-Boc solid phase peptide synthesis system [7]. A tyrosine residue (shown in

Please cite this article in press as: Patarroyo ME, et al. Biological and structural characteristics of the binding peptides from the sporozoite proteins essential for cell traversal (SPECT)-1 and -2. Peptides (2010), doi:10.1016/j.peptides.2010.09.026

italics and underlined through the text and in Fig. 1B) was added to the C-terminus of those peptides lacking it to allow radiolabeling, as thoroughly described [5,13,20]. To predicted B-cell epitopes (see below) CG and GC residues were added at the N and C termini, respectively, to obtain peptide polymers by oxidation, as described elsewhere [3,4,14,16].

2.2. Production of anti-SPECTs antibodies in rabbits

The complete sequences of SPECT-1 and SPECT-2 were analyzed with the BCPREDS (http://ailab.cs.iastate.edu/bcpred/index.html) and BcePred (http://www.imtech.res.in/raghava/bcepred/) prediction servers in order to identify specific B-cell epitopes. Two New Zealand rabbits were subcutaneously inoculated with one of the following 2 mixtures of polymeric peptides: mixture A, containing SPECT-1 peptides 37339 (CG^{44}DVEDDSKNEIVDNIQKMVDD^{63}GC) and 37340 (CG^{209}NNDDIKEIELVNFISTNYDK^{228}GC), or mixture B, containing SPECT-2 peptides 37343 (CG^{121}NNSDEEQIENSNNNNSDEEQ^{140}GC) and 37344 (CG^{201}DKEKRLNFNGDQKDEDNEEN^{220}GC) (Fig. 1B, in blue). Peptides were emulsified in Freund's complete adjuvant for the first dose delivered on day 1, and in incomplete Freund's adjuvant for the second and third doses delivered on days 21 and 41, respectively. Serum samples were collected pre-immunization and 40 and 60 days later, to evaluate antibody production.

2.3. Indirect immunofluorescence assays (IFA)

The reactivity of rabbits antisera against SPECT-1 (mixture A) or SPECT-2 (mixture B) peptides, used as the first antibody, was characterized by IFA analysis using *P. falciparum* sporozoites (3D7 strain) kindly provided by Dr. Patricia de la Vega (Naval Institute Bethesda, MD, USA), as previously described [3,5,16]. Their reactivities were detected with goat-antirabbit IgG, affinity purified and conjugated with Fluoresceine Isothiocyanate (FITC), emitting a green fluorescent color under UV microscopy. Co-localization was performed with *Aotus* monkey's anti CSP 24258 modified peptide (derived from 4383 conserved HABP) [3] used as second antibody, and detected with goat anti *Aotus* IgG; the F(ab)2 fragment was affinity purified and conjugated with Rhodamine Isothiocyanate (RITC), which gives a red color in the fluorescence microscope (Fig. 1A).

2.4. Production of HeLa cells

HeLa cells were grown as a confluent monolayer in RPMI 1640 medium supplemented with 10% fetal bovine serum (Gibco). Cells were detached from the tissue-culture flask using 0.05% EDTA–PBS solution, washed with incomplete medium, stained with trypan blue and counted in a Neubauer chamber.

2.5. Binding assays with SPECT-1 and SPECT-2 peptides

Binding assays to HeLa cells were performed according to described protocols [5,20]. Briefly, HeLa cells (1.2×10^6 cells) were incubated with increasing concentrations of radiolabeled SPECT-1 and SPECT-2 peptides, in the absence (total binding) or the presence (unspecific binding) of high concentrations (400×) of unlabeled peptide for 1 h. Then, the reaction mixture was centrifuged at $15{,}000 \times g$ for 3 min through a 60:40 dioctyl phthalate/dibutyl phthalate cushion (1.015 g/mL density), the supernantant was discarded and the cell-associated radioactivity was quantified in a gamma counter (Gamma Counter Cobra II). All assays were performed in triplicate. Those peptides having an activity greater than or equal to 2% (0.02 ratio) were considered high-activity binding peptides (HABPs), according to previously established criteria [3–5,17,20].

In addition, a modified binding assay employing a wider range of radiolabeled peptide concentrations was performed to determine the dissociation constant (K_d), number of binding sites per cell (BSC) and Hill coefficients (n_H) [5,20] of SPECT-1 and SPECT-2 HABPs.

2.6. Binding assays with enzymatically treated HeLa cells

HeLa cells (4×10^4 cells/μL) suspended in HBS were treated for 1 h at 37 °C with 750 μU/mL of one of the following enzymes: Heparinase I (HI; CAS 9025-39-2, Sigma), Heparinase II (HII; CAS 149371-12-0, Sigma), chondroitinase AC (CAC; CAS 9047-57-8, Sigma) and chondroitinase ABC (CABC; CAS 9024-13-9, Sigma) [19], according to the manufacturer's instructions. Cells were then washed and used to perform conventional binding assays with SPECT-1 and SPECT-2 HABPs. Untreated cells were used as control (100% binding).

2.7. CD spectroscopy

Circular dichroism spectra of SPECT-1 and SPECT-2 HABPs in 30% (v/v) trifluoroethanol (TFE) were recorded at 20 °C using a Jasco J-810 (JASCO INC.) equipment. Spectra were acquired by averaging three sweeps taken at 20 nm/min. Data were processed using Spectra Manager software and analyzed with CONTINLL, SELCON, and CDSSTR deconvolution programs [23].

2.8. NMR analysis

Ten milligrams of 34936, 34938, 34941, 34949 and 34951 SPECT-2 HABPs, theoretically localized in the MACPF 3D structure's domain, were dissolved in 500 μL TFE-d3/H_2O (30/70, v/v) to record their spectra in a BRUKER DRX-500 spectrometer at 295 K. The basic NMR structure determination protocol was as follows: proton spectra were assigned by DQF-COSY, TOCSY, and NOESY; TOCSY and DQF-COSY spectra were then used to identify individual spin systems (amino acids) and NOESY (400 ms mixing time) to identify stretches of amino acids within a given primary (sequential assignment) and secondary structure. TOCSY spectra recorded at different temperatures (285–315 K) were used to obtain amide temperature coefficients for predicting hydrogen bonds ($-\Delta\delta H^N/\Delta T$, ppb/K), as thoroughly described before [26].

2.9. Structure calculations

NOESY peak signals were classified as strong (1.8–2.5 Å), medium (2.5–3.5 Å), and weak (3.5–5.0 Å), according to their relative intensity. Hydrogen bond constraints were introduced for low amide temperature coefficients: only <4 and $-\Delta\delta H^N/\Delta T$, ppb/K were used in structure calculations. Distance ranges involving these likely NH–O hydrogen bonds were set at 1.8–2.5 Å, between a residue acceptor oxygen ($i-4$) and a residue donor amide hydrogen (i). A family of 50 structures was obtained using Distance Geometry software (DGII) and then refined using simulated annealing protocol (DISCOVER software), to select those having reasonable geometry and fewer violations.

3. Results

3.1. Anti-SPECT-1 and Anti-SPECT-2 sera recognize surface and micronemal-contained molecules

Immunofluorescence assays with anti-SPECT-1 (mixture A) or anti-SPECT-2 (mixture B) rabbit sera detected a protein on the parasite's surface and in small intracytoplasmic granules (green fluorescence); suggestive of its micronemal origin and

Please cite this article in press as: Patarroyo ME, et al. Biological and structural characteristics of the binding peptides from the sporozoite proteins essential for cell traversal (SPECT)-1 and -2. Peptides (2010), doi:10.1016/j.peptides.2010.09.026

further translocation to the sporozoite's membrane (Fig. 1A). Pre-immune sera did not show any fluorescence (data not shown). Co-localization with *Aotus* sera produced against the *P. falciparum* CSP modified HABP, displayed the same Immunofluorescence pattern on the sporozoite's membrane, as well as the small intracytoplasmic structures (red), suggesting once more the micronemal origin and membranal translocation of these molecules.

3.2. SPECT-1/-2 peptides specifically interact with HeLa cells

Binding assays were conducted to identify the binding regions of SPECT-1 and SPECT-2, interacting specifically with HeLa cells. Three peptides showing high specific binding activities (therefore denoted as HABPs) were localized in the central region of SPECT-1 (HABPs 33372 ^{88}ASLEEVSDHVVQNISKYSLT^{107}, 33374 ^{129}LISNLSKRQQKLKGDKIKKVY^{148} and 33375 ^{149}TDLILKKLKKLENVNKLIKY^{168}) (Fig. 1B), while 14 (Fig. 1B) were identified in SPECT-2.

In SPECT-2, the HABPs defined three regions of high specific binding activity: a first cysteine-rich region, encompassing residues 21–260 and containing HABP 34925 (^{61}VLCNSILC KNDKISSFINQRY^{80}) (Fig. 1B), a second region, spanning residues 261–600 and containing 8 HABPs included within the MACPF-related domain (HABPs 34935 ^{261}EADSLIDPGYRAQIYLMEWA^{280}, 34936 ^{281}LSKEGIANDLSTLQPVNGWIY^{300}, 34938 ^{321}YTKSLSAEAKVSGSYWGIAS^{340}, 34939 ^{341}FSASTGYSSFLHEVTKRSKK^{360}, 34941 ^{381}WDKTTAYKNAVNELPAVFTG^{400}, 34946 ^{481}SAGGSTDVNSSNSSANDEQSY^{500}, 34949 ^{541}KLTPISDSFDSDDLKESYDK^{560}, 34951 ^{581}DKDIIKILTNADTVTKNSAPY^{600}); this region has been associated with the sporozoite cell-traversal activity mediated by SPECT-2 [8,9,11], and finally a third cysteine-rich region, extending from residue 601 to 842 (Fig. 1B) and containing 5 HABPs (34953 ^{621}NFWDNTNALKGYNIEVCEAG^{640}, 34957 ^{701}SSSGRINSAEYVYSTPCIPG^{720}, 34958 ^{721}MKSCSLNMNNDNQKSYIYVL^{740}, 34959 ^{741}CVDTTIWSGVNNLSLVALDGY^{760}, 34960 ^{761}AHGKVNRSKKYSDGELVGTC^{780}), each of which contained one cysteine residue (shown in italics above).

SPECT-1 and SPECT-2 HABPs recognized between 80,000 and 300,000 binding sites per cell, showed K_d values within the nanomolar range and n_H values higher than 1.0, as determined by Hill analysis (Table 1).

3.3. SPECT-1 and SPECT-2 HABPs interact with sulfated proteoglycans

The nature of the receptor(s) for SPECT-1 and SPECT-2 HABPs was analyzed in binding assays with enzymatically treated HeLa cells. In SPECT-1, binding of HABP 33372 was only affected by treatment with CABC, while HI and HII had a more prominent effect on the interaction of HABP 33374 with HeLa cells. Strikingly, HABP 33375 binding was dramatically affected by all enzymatic treatments (Table 1).

In SPECT-2, treatment of HeLa cells with HI and CAC diminished (in some circumstances almost abolished) most interactions with HABPs (except for HABP 34951 and 34960). Treatment with CABC also diminished binding of SPECT-2 HABPs 34939 and 34951, while binding of HABP 34949 was highly reduced by all enzymatic treatments (Table 1).

3.4. CD spectroscopy

CD studies conducted to analyze the secondary structures of SPECT-1 and SPECT-2 HABPs showed a high content of α-helical elements in HABPs 33372, 33374 and 33375 structures from SPECT-1, as indicated by the two typical minima at 206 and 221 nm. The majority of SPECT-2 HABPs showed typical α-helical spectra, except for HABPs 34938, 34953, 34958 and 34960, which showed displacements associated with the presence of some other structural elements, such as β-turns and/or random coils (Fig. 1C). These results were in agreement with deconvolution analyses for SPECT-1 and most of SPECT-2 HABPs (data not shown).

3.5. NMR assignment

Cross-peaks between NH and CHα protons were identified by analyzing COSY spectra acquired in 30% TFE-d3/H_2O. TOCSY spectra were used to correlate side-chain spin-systems with NH–CHα cross-peaks, following Wüthrich's methodology for the assignments [26]. In each HABP, strong and medium NOEs were found for $d_{\alpha N}$ (i, $i+1$) connectivities throughout the whole peptide chain (Supplemental Material).

The NOESY spectra of SPECT-2 HABPs 34936, 34941 and 34951 showed medium range $d_{\alpha\beta}$ (i, $i+3$), $d_{\alpha N}$ (i, $i+3$), $d_{\alpha N}$ (i, $i+4$) NOE connectivities, suggesting the presence of α-helical structures. HABP 34936 showed three short α-helical fragments between residues K3–I6, D9–T12 and V16–W19, while HABP 34941 showed an α-helix between A6 and E13, and HABP 34951 between K2 and Y18. HABP 34949 displayed $d_{\alpha N}$ (i, $i+3$), $d_{\alpha N}$ (i, $i+4$) but not $d_{\alpha\beta}$ (i, $i+3$) NOE connectivities, indicating a random structure as suggested by CD studies, with the presence of a distorted α-helix between S6 and F9. HABP 34938 had a totally extended form due to the absence of medium range signals (Supplementary material).

Table 1
Binding constants of SPECT-1 and SPECT-2 HABPs and percentage binding activities to HeLa cells treated with different enzymes.

	Binding constants[a,b]				Binding to treated cells[a,c] (%)			
	HABP	K_d (nM)	n_H	BSC	HI	HII	CAC	CABC
SPECT-1	33372	850	1	84,000	105	104	190	48
	33374	750	1.4	241,000	62	54	91	70
	33375	750	1.7	281,000	19	22	21	23
SPECT-2	34925	680	2.9	36,000	0.1	132	0.0	140
	34936	ND	ND	ND	54	98	46	101
	34938	770	1.9	19,000	ND	ND	ND	ND
	34939	870	1.7	360,000	0.1	118	0.0	47
	34949	750	1.1	68,000	12	46	43	47
	34951	ND	ND	ND	77	84	78	37
	34958	460	1.8	34,000	49	62	15	180
	34959	600	1.8	30,000	34	170	18	115
	34960	ND	ND	ND	49	99	85	87

[a] All standard deviations were below 10%.
[b] K_d: Dissociation constants; n_H: Hill coefficients; BSC: binding sites per cell.
[c] Bindings that were significantly affected by a particular enzymatic treatment are shown in bold ND: non-assessed peptide.

Please cite this article in press as: Patarroyo ME, et al. Biological and structural characteristics of the binding peptides from the sporozoite proteins essential for cell traversal (SPECT)-1 and -2. Peptides (2010), doi:10.1016/j.peptides.2010.09.026

3.6. Structure calculations

Fifty structures were initially calculated for SPECT-2 HABPs 34936, 34941, 34949 and 34951 and the best-fitting backbone (N, Cα, C) atom superimpositions, showing no distance violations greater than 0.3 Å and ω angles greater than 1.5°, were selected (see Section 2.9). The previously described structural features were confirmed by the medium-range NOEs and by the dihedral Φ and Ψ angles of each residue in the helical region adopting equal values (approximately −60° and 45°, respectively). The carboxy and amino terminal regions were flexible (Fig. 1D).

4. Discussion

Traversal of Kupffer cells in the liver is critical for sporozoite invasion of hepatocytes. Among the set of surface proteins involved in this process, the sporozoite micronemal proteins SPECT-1 and SPECT-2 are extremely important, since the cell-traversal activity is completely abolished when parasites are genetically knocked down in these proteins [1,2,8,9,11,27].

Here, we have determined the binding profiles of the peptides encompassing the complete sequences of SPECT-1 and SPECT-2, with the aim of identifying specific HABPs for HeLa cells that might be directly involved in the cell traversal ability of sporozoites [1,8,9,11,27]. As a result, three HABPs were identified in the central region of SPECT-1 and 14 were found to define three binding regions in SPECT-2 (Fig. 1B), as described in Section 3.2. The high affinity interactions between SPECT-1 and SPECT-2 HABPs and HeLa cells were demonstrated by their nanomolar K_d and the recognition of 80,000–300,000 binding sites per cell in saturation assays. In addition, Hill analyses (Table 1) indicated that there is positive cooperativity in the binding interactions of all HABPs, as suggested by their n_H values, higher than 1.0.

Remarkably, there is high sequence conservation in SPECT-1 and SPECT-2 HABPs among the different parasite strains available in the PlasmoDB server (http://plasmodb.org/plasmo/), with only SPECT-1 HABP 33372 showing a limited genetic variability. This high degree of conservation makes them attractive targets for a fully effective antimalarial vaccine design, able to overcome undesirable strain-specific immune responses.

The immunological potential of SPECT HABPs was analyzed in IFA assays, using rabbit anti-SPECT-1 and anti-SPECT-2 antisera produced against chemically synthesized B cell epitopes. The surface and micronemal distribution observed with both antisera (Fig. 1A), as well as the co-localization studies with anti-CSP antibodies agree with the previously reported micronemal localization of SPECT-1 and SPECT-2, as well as with their further translocation to sporozoite surface after leaving the mosquito's salivary glands to mediate hepatocyte invasion, as described for CSP and TRAP [8,11,14]. Unfortunately, recombinant SPECT-1 or SPECT-2 proteins are not available to us to perform confirmatory Western blot analyses.

Since specific interactions between highly relevant sporozoite proteins like CSP and TRAP with host's cell surface proteoglycans have been clearly established [12,19,24], the nature of the HeLa surface receptors for SPECT-1 and SPECT-2 HABPs was explored by analyzing the effect of treating cells with HI, HII, CAC or CABC on the capacity of HABPs to bind HeLa cells. These enzymes act differentially on specific cell surface proteoglycans: HI and HII cleave heparin-like oligosaccharides with high or low content of sulfate groups, respectively, while CAC acts on chondroitin-6-sulfate, chondroitin-4-sulfate and chondroitin-4,6-sulfate, and CABC cleaves chondroitin-containing molecules plus dermatan sulfate [19].

Regarding SPECT-1, the diminished binding activity of HABP 33372 caused by CABC suggests its interaction with dermatan-containing receptors, while the sensitivity of the HABP 33374–HeLa cell interaction to HI and HII could be associated with binding to surface molecules containing heparin-like (Table 1). Moreover, binding of HABP 33375 is likely to be recognizing heparin-like, chondroitin-like and/or dermatan-sulfate oligosaccharides on the surface of HeLa cells [19], since its binding is affected by all enzymatic treatments (Table 1).

On the other hand, a marked sensitivity was evidenced in practically all SPECT-2 HABPs binding to HeLa cells treated with HI and CAC (only the binding activities of HABPs 34951 and 34960 were resistant) (Table 1), which could be suggesting specific interactions with heparin high- and chondroitin sulfate-carrying surface molecules. Furthermore, HABPs 34939, 34949 and 34951 could also be associated with receptors containing dermatan-like [19] since their binding activities were also affected by CABC (Table 1).

These results, together with the ones previously described for CSP [19], strongly suggests that SPECT-1, SPECT-2 and CSP could be using similar host cell surface receptors to mediate cell traversal processes. Additionally, the different behaviors shown in assays with heparinase- and chondroitinase-treated cells might be related to the use of alternative pathways for cell recognition and traversal, but this should be further explored.

Studies conducted with the aim of designing a fully effective antimalarial vaccine with the most important *P. falciparum* merozoite (the RBC invasive form of the parasite) proteins, and more recently with the leading antimalarial candidates CSP [3] and TRAP [16], the sporozoite and liver stage antigen (SALSA) and the liver stage antigen-1 (LSA-1) [4], have lead to establish the undeniable relevance of conducting structural analysis on all *P. falciparum* non-immunogenic conserved HABPs, since they can become new and very potent protection inducing vaccine components, once being specifically modified [14,17]. Accordingly, CD deconvolution studies were performed on SPECT-1 and SPECT-2 HABPs, finding a high content of α-helical features in SPECT-1 HABPs, while some SPECT-2 HABPs displayed α-helical structures and others displayed different structural features (β-turns and/or random coils) (Fig. 1C).

The MACPF domain, originally identified by its amino-acid sequence homology within the Complement cascade proteins C6, C7, C8α, C8β, C9 and perforin complex, is present in a large family of evolving ancient disparate proteins, using a similar architecture to damage membranes, which include the cholesterol dependent cytolisins (CDCs) of Gram-positive or Gram-negative bacteria, the BCL family of apoptosis regulator and the MACPF family of the apicomplexa parasites (malaria, Toxoplasma, Babesia) among others [10].

The membrane damage is characterized in the CDCs proteins by oligomerization and assembly of the individual subunits into a ring-shaped-pore that inserts into membranes to form a large amphipatic transmembrane β barrel. Although MACPF and CDCs are very divergent at the aminoacid sequence level, they display a common fold and a very similar membrane disruption mechanism [21].

The MACPF/CDC canonical 3D structure posses an N-terminal region of variable length, followed by the centrally located MACPF domain of ~40 kDa, ending in a β-pleated-rich domain, unique to apicomplexa. These parasitic MACPF-like-containing proteins (among them *P. falciparum* SPECT-2) are localized in the micronemes, to be translocated to the parasite membrane during host cell invasion. The recently described C8α MACPF and CDC 3D structures by X-ray crystallography, revealed that they share specific structural characteristics such as being flattened with a central kinked four-stranded β sheet core region, surrounded by α-helix and β-turns that define different domains, [6,25]. Among these four domains (D1 to D4) of the CDC structure, D4 binds to membranes, while D2 links D1 to D3, the last two mediating membrane insertion and pore formation [6] (Fig. 1D, left panel, MACPF

Please cite this article in press as: Patarroyo ME, et al. Biological and structural characteristics of the binding peptides from the sporozoite proteins essential for cell traversal (SPECT)-1 and -2. Peptides (2010), doi:10.1016/j.peptides.2010.09.026

lateral and frontal views). MACPF-domain containing proteins also share special signatures like the Y/WGT/SHF xxxxxxGG (present in SPECT-2 peptides 35558 and 34944) and KN motives (present in HABPs 34941 and 34951), suggested to be involved in host's cell membrane binding.

Strikingly, when SPECT-2 HABPs showing similar amino acid sequences were structurally compared to their corresponding segments in the C8α MACPF domain, they also displayed similar structural elements, as indicated by deconvolution analyses of CD spectra (Fig. 1C2 and C3) or when their ^{1}H NMR 3D structures were superimposed onto their analogous MACPF sequences (Fig. 1D).

In this way, the 3D structure of the fragment containing HABP 34938 (dark blue, Fig. 1D, left panel) displays an extended configuration similar to the random structure shown by CD (Fig. 1C3), while the α-helical configuration shown by HABP 34939 in deconvolution analysis correlates very well with the 3D structural element determined in the C8α segment (brown, Fig. 1D, left panel), located at the beginning of the MACPF central β sheet-rich region.

More convincing, the α-helical A6–E13 region of HABP 34941 (yellow ribbon, Fig. 1D, right panel) determined by ^{1}H NMR displays an RMSD of 0.81 when being superimposed with the corresponding C8α MACPF fragment (green, Fig. 1D, left panel). Similarly, the 3D structure of HABP 34951 (gray ribbon, Fig. 1D, right panel), helical between K2–Y18 when superimposed onto the C8α MACPF 3D structure (red ribbon, Fig. 1D, left panel), displays an RMSD of 0.52, demonstrating almost identical structure between HABPs 34941 and 34951 with the C8α MACPF regions, mediators of membrane insertion and pore formation. HABP 34949 (dark blue, Fig. 1D, right panel) can be superimposed with its corresponding C8α MACPF portion (purple, Fig. 1D, right panel) with an RMSD of 4.5, suggesting similar but not identical structural characteristics.

Some structural differences between SPECT-2 and C8α MACPF could only be observed in HABP 34935 (pink in the 3D structure, Fig. 1D, left), which showed a short α-helix in the 3D C8α MACPF structure, while being completely α-helical in CD analyses (Fig. 1C2), and HABP 34936 (orange structure obtained by ^{1}H NMR, Fig. 1D, right), which displayed a high α-helical content in contrast to the partially α-helical and random coil structures found in the C8α MACPF 3D structure. Unfortunately, the C8α MACPF region corresponding to SPECT-2 HABP 34946, being α-helical by CD analysis, was not elucidated in the C8α structure determined by X-ray crystallography. Interestingly, HABPs 34941 and 34951 (both α-helical) contain the KN sequence (boxed in Fig. 1B), a putative sulfate binding sequence described for CDCs [18], which could be associated with the interaction of SPECT-2 with highly sulfated proteoglycans on the surface of mammalian host cells (chondroitin and dermatan sulfate receptors), as corroborated by the enzymatic sensitivity of the binding capacity of SPECT-2 HABPs (Table 1).

We have recently shown that in conserved HABPs (like 34941 and 34951), those residues (like KN) specifically interacting with receptor molecules, are the critical binding residues that need to be modified to render these non-immunogenic, non-protection inducer, functionally relevant conserved HABPs into sterile immunity inducer peptides [15], making these two SPECT-2 HABPs excellent candidates to be included as components of a fully effective antimalarial vaccine. Other HABPs like 34949, embedded in the MACPF structure, could be also excellent prospects, due to the demonstrated high sensitivity to all enzymatic treatments (Table 1).

The amino acid sequence similarity (13% identity plus 30% similarity) between the SPECT-2 and C8α MACPF homologue domains, together with the high similarity at the secondary and tridimensional structural level (Fig. 1D) in their functionally relevant segments, lead us to suggest a 3D structural conservation of the SPECT MACPF domain and their homologue C8α MACPF and CDC membrane-pore-forming proteins, which could be associated with the previously reported function of this domain and SPECT-2 in pore formation and cell traversal mechanisms [8,9,11].

We have shown here the identification of sequences derived from the cell traversal-associated SPECT-1 and SPECT-2 proteins with specific binding activity to HeLa cells, most of which display high affinity for heparin and chondroitin sulfate-containing receptors, as determined by enzymatic treatments, same as reported for other sporozoite proteins involved in cell traversal. SPECT-2 MACPF-related HABPs display high similarity at the primary, secondary and tertiary structure with the C8α and CDC pore-forming protein family (as shown here), highlighting the potential of SPECT-1 and SPECT-2 HABPs as attractive targets to be further included as antigens in the search of a multi-stage, multi-antigenic, minimal subunit-based, chemically synthesized fully effective vaccine against *P. falciparum* malaria.

Acknowledgements

To Jeison Garcia and Gabriela Arevalo who participated at the beginning of this work, and Gisselle Rivera for her collaboration in the translation of this manuscript.

Appendix A. Supplementary data

Supplementary data associated with this article can be found, in the online version, at doi:10.1016/j.peptides.2010.09.026.

References

[1] Akhouri RR, Sharma A, Malhotra P, Sharma A. Role of *Plasmodium falciparum* thrombospondin-related anonymous protein in host–cell interactions. Malaria journal 2008;7:63.
[2] Amino R, Giovannini D, Thiberge S, Gueirard P, Boisson B, Dubremetz JF, et al. Host cell traversal is important for progression of the malaria parasite through the dermis to the liver. Cell Host & Microbe 2008;3:88–96.
[3] Bermudez A, Vanegas M, Patarroyo ME. Structural and immunological analysis of circumsporozoite protein peptides: a further step in the identification of potential components of a minimal subunit-based, chemically synthesised antimalarial vaccine. Vaccine 2008;26:6908–18.
[4] Cifuentes G, Vanegas M, Martinez NL, Pirajan C, Patarroyo ME. Structural characteristics of immunogenic liver-stage antigens derived from *P. falciparum* malarial proteins. Biochemical and Biophysical Research Communications 2009;384:455–60.
[5] Garcia JE, Puentes A, Patarroyo ME. Developmental biology of sporozoite-host interactions in *Plasmodium falciparum* malaria: implications for vaccine design. Clinical Microbiology Reviews 2006;19:686–707.
[6] Hadders MA, Beringer DX, Gros P. Structure of C8alpha-MACPF reveals mechanism of membrane attack in complement immune defense. Science (New York, NY) 2007;317:1552–4.
[7] Houghten RA. General method for the rapid solid-phase synthesis of large numbers of peptides: specificity of antigen-antibody interaction at the level of individual amino acids. Proceedings of the National Academy of Sciences of the United States of America 1985;82:5131–5.
[8] Ishino T, Chinzei Y, Yuda M. A Plasmodium sporozoite protein with a membrane attack complex domain is required for breaching the liver sinusoidal cell layer prior to hepatocyte infection. Cellular Microbiology 2005;7:199–208.
[9] Ishino T, Yano K, Chinzei Y, Yuda M. Cell-passage activity is required for the malarial parasite to cross the liver sinusoidal cell layer. PLoS Biology 2004;2:E4.
[10] Kafsack BF, Carruthers VB. Apicomplexan perforin-like proteins. Communicative & Integrative Biology 2010;3:18–23.
[11] Kaiser K, Camargo N, Coppens I, Morrisey JM, Vaidya AB, Kappe SH. A member of a conserved Plasmodium protein family with membrane-attack complex/perforin (MACPF)-like domains localizes to the micronemes of sporozoites. Molecular and Biochemical Parasitology 2004;133:15–26.
[12] Kappe SH, Buscaglia CA, Nussenzweig V. Plasmodium sporozoite molecular cell biology. Annual Review of Cell and Developmental Biology 2004;20:29–59.
[13] Lopez R, Valbuena J, Rodriguez LE, Ocampo M, Vera R, Curtidor H, et al. *Plasmodium falciparum* merozoite surface protein 6 (MSP-6) derived peptides bind erythrocytes and partially inhibit parasite invasion. Peptides 2006;27:1685–92.
[14] Patarroyo ME, Cifuentes G, Bermudez A, Patarroyo MA. Strategies for developing multi-epitope, subunit-based, chemically synthesized anti-malarial vaccines. Journal of Cellular and Molecular Medicine 2008;12:1915–35.
[15] Patarroyo ME, Cifuentes G, Martinez NL, Patarroyo MA. Atomic fidelity of subunit-based chemically-synthesized antimalarial vaccine components. Progress in Biophysics and Molecular Biology 2010;102:38–44.

Please cite this article in press as: Patarroyo ME, et al. Biological and structural characteristics of the binding peptides from the sporozoite proteins essential for cell traversal (SPECT)-1 and -2. Peptides (2010), doi:10.1016/j.peptides.2010.09.026

[16] Patarroyo ME, Cifuentes G, Rodriguez R. Structural characterisation of sporozoite components for a multistage, multi-epitope, anti-malarial vaccine. The International Journal of Biochemistry & Cell Biology 2008;40:543–57.
[17] Patarroyo ME, Patarroyo MA. Emerging rules for subunit-based, multiantigenic, multistage chemically synthesized vaccines. Accounts of Chemical Research 2008;41:377–86.
[18] Polekhina G, Giddings KS, Tweten RK, Parker MW. Insights into the action of the superfamily of cholesterol-dependent cytolysins from studies of intermedilysin. Proceedings of the National Academy of Sciences of the United States of America 2005;102:600–5.
[19] Pradel G, Garapaty S, Frevert U. Proteoglycans mediate malaria sporozoite targeting to the liver. Molecular Microbiology 2002;45:637–51.
[20] Rodriguez LE, Curtidor H, Urquiza M, Cifuentes G, Reyes C, Patarroyo ME. Intimate molecular interactions of *P. falciparum* merozoite proteins involved in invasion of red blood cells and their implications for vaccine design. Chemical Reviews 2008;108:3656–705.
[21] Rosado CJ, Kondos S, Bull TE, Kuiper MJ, Law RH, Buckle AM, et al. The MACPF/CDC family of pore-forming toxins. Cellular Microbiology 2008;10:1765–74.
[22] Snow RW, Guerra CA, Noor AM, Myint HY, Hay SI. The global distribution of clinical episodes of *Plasmodium falciparum* malaria. Nature 2005;434:214–7.
[23] Sreerama N, Venyaminov SY, Woody RW. Estimation of protein secondary structure from circular dichroism spectra: inclusion of denatured proteins with native proteins in the analysis. Analytical Biochemistry 2000;287:243–51.
[24] Tossavainen H, Pihlajamaa T, Huttunen TK, Raulo E, Rauvala H, Permi P, et al. The layered fold of the TSR domain of *P. falciparum* TRAP contains a heparin binding site. Protein Science 2006;15:1760–8.
[25] Tweten RK. Cholesterol-dependent cytolysins, a family of versatile pore-forming toxins. Infection and Immunity 2005;73:6199–209.
[26] Wüthrich K. NMR of Protein and Nucleic Acids. New York: Wiley; 1986.
[27] Yuda M, Ishino T. Liver invasion by malarial parasites—how do malarial parasites break through the host barrier? Cellular Microbiology 2004;6:1119–25.

Please cite this article in press as: Patarroyo ME, et al. Biological and structural characteristics of the binding peptides from the sporozoite proteins essential for cell traversal (SPECT)-1 and -2. Peptides (2010), doi:10.1016/j.peptides.2010.09.026

ANEXO 2

Región de Interacción HN*i* - HN*i+1*

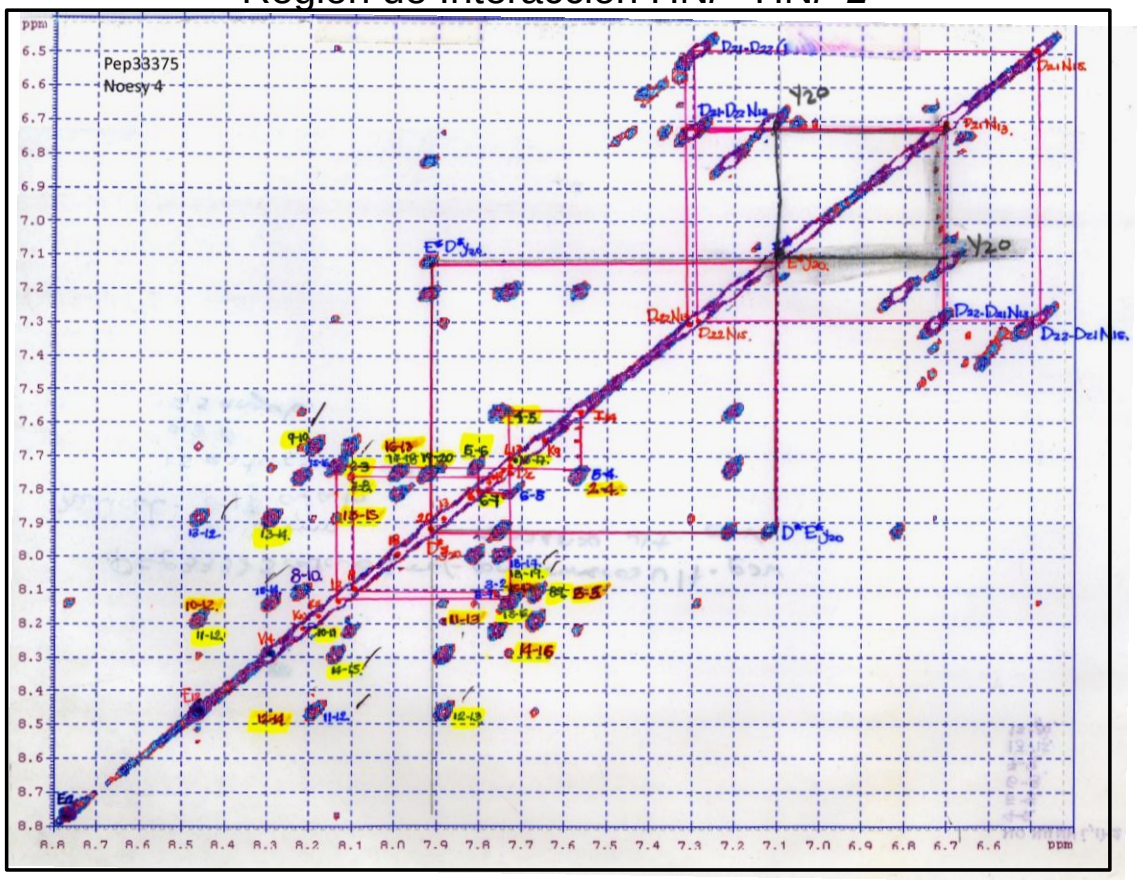

ANEXO 3

Protocolo “Simulated Annealing”

“Simulated Annealing” (SA) es un proceso de simulación de desorden restringido mediante el cual se fuerzan a los átomos de la molécula a que ocupen posiciones posibles en el espacio, se les da la energía necesaria para que salten barreras de energía (Dinámica Molecular restringida) y después por procesos de Minimización de Energía a que lleguen a estructuras estables.

El protocolo de SA incluye las siguientes fases:

1- Elevar la Temperatura a 1000K por 12 ps en tres fases. La constante de fuerza que se usa es de 0.001 a 30 Kcal.

2- Enfriamiento a 300 K en dos estados.

3- Minimización de energía en cuatro fases. 100 pasos de “steepest descendent”, 1000 pasos de gradiente conjugado (hasta llegar a un derivativo de 0.1), 100 pasos de “steepest descendent” (hasta llegar a la derivada de 0.01) y 2000 pasos en gradiente conjugado (hasta llegar a un derivativo de 0.01).

ANEXO 4

Alineamiento del dominio MACPF de la proteína SPECT-2 y el dominio MACPF del factor de complemento C8α. En colores se muestra la localización de los péptidos de alta capacidad de unión a células HeLa.

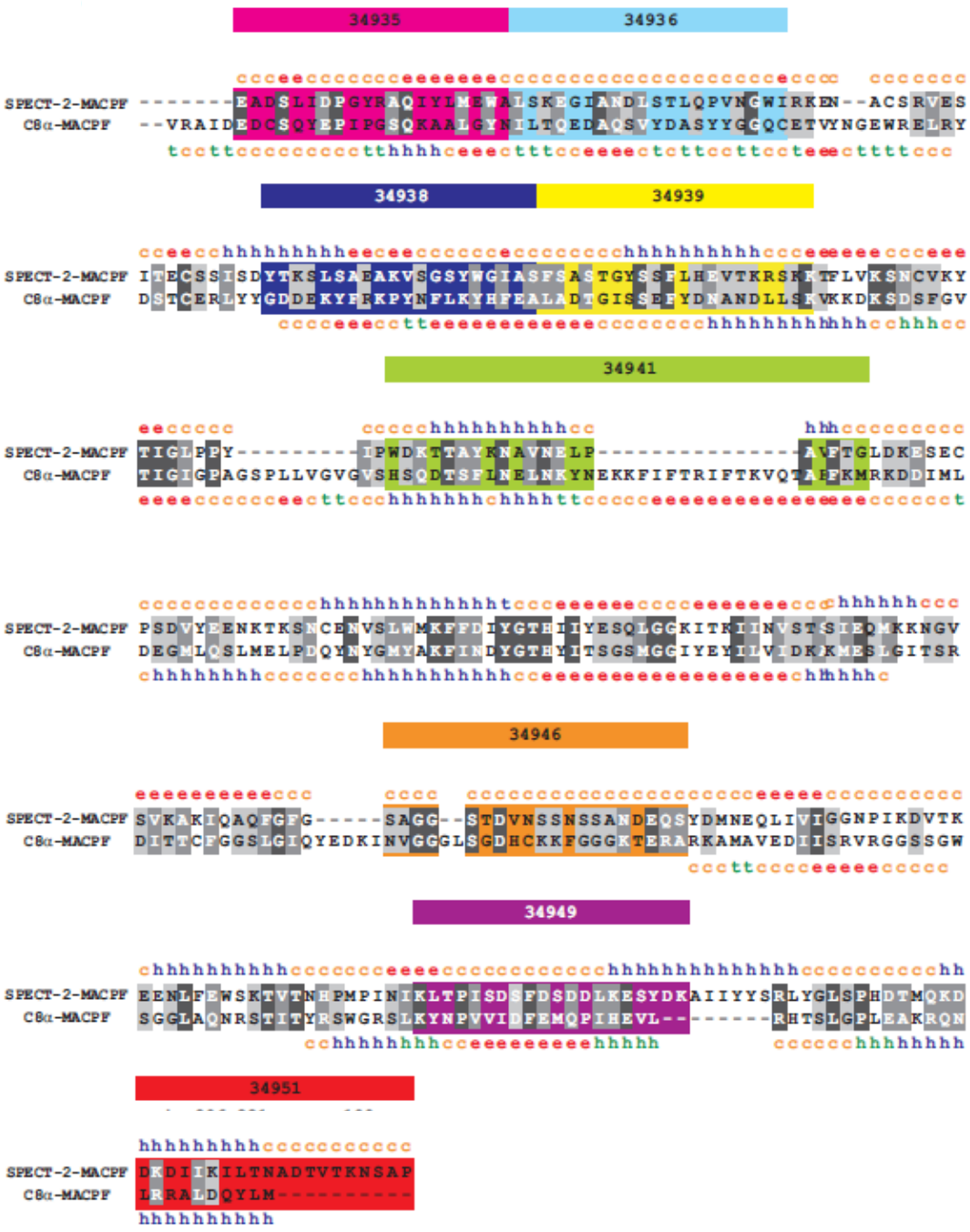

ANEXO 5

Alba MP, Suarez CF, Varela Y, Patarroyo MA, Bermudez A, Patarroyo ME. TCR-contacting residues orientation and HLA-DRβ* binding preference determine long-lasting protective immunity against malaria. BBRC. 2016. 477:654-670

Contents lists available at ScienceDirect

Biochemical and Biophysical Research Communications

journal homepage: www.elsevier.com

TCR-contacting residues orientation and HLA-DRβ* binding preference determine long-lasting protective immunity against malaria

Martha P. Alba [a, b, c], Carlos F. Suarez [a, b], Yahson Varela [a], Manuel A. Patarroyo [a, b, d], Adriana Bermudez [a, b], Manuel E. Patarroyo [a, d, *]

[a] *Fundación Instituto de Inmunología de Colombia (FIDIC), Bogotá D. C., Colombia*
[b] *Universidad del Rosario, Bogotá D. C., Colombia*
[c] *Universidad de Ciencias Aplicadas y Ambientales (UDCA), Bogotá, Colombia*
[d] *Universidad Nacional de Colombia, Bogotá D. C., Colombia*

ARTICLE INFO

Article history:
Received 22 June 2016
Accepted 23 June 2016
Available online xxx

Keywords:
Antimalarial-vaccine
T-cell-receptor
MHC-II
Immunological memory
Rotamer-orientation

ABSTRACT

Fully-**p**rotective, **l**ong-**l**asting, **i**mmunological (FPLLI) memory against *Plasmodium falciparum* malaria regarding **im**mune **p**rotection-**i**nducing **p**rotein **s**tructures (IMPIPS) vaccinated into monkeys previously challenged and re-challenged 60 days later with a lethal *Aotus* monkey-adapted *P. falciparum* strain was found to be associated with preferential high binding capacity HLA-DRβ1* allelic molecules of the **m**ajor **h**istocompatibility **c**lass **II** (MHC-II), rather than HLA-DRβ3*, β4*, β5* alleles. Complete $PPII_L$ 3D structure, a longer distance (26.5 Å ± 1.5 Å) between residues perfectly fitting into HLA-DRβ1*PBR pockets 1 and 9, and a *gauche*$^-$ rotamer orientation in p8 TCR-contacting polar residue and a larger volume of polar p2 residues was also found. This data, in association with previously-described p3 and p7 apolar residues having *gauche*$^+$ orientation to form a perfect MHC-II-peptide-TCR complex, determines the stereo-electronic and topochemical characteristics associated with FPLLI immunological memory.

1. Introduction

One of the main problems in vaccine development is the induction of FPLLI memory. Microbes (viruses, bacteria, parasites, etc.) have developed an incredible number of escape mechanisms against immune pressure, such as antigenic diversity where a single amino acid (aa) mutation or replacement can completely avert previously developed immunity, as occurs with *Plasmodium falciparum* malaria proteins apical membrane antigen-1 (AMA-1) [1,2], merozoite surface protein-1 (MSP-1) [3], etc., to quote a few. Microbes can also induce suppression, blocking [4], impeding [5,6] and many other escape mechanisms [7] rendering new or previously acquired immunity useless.

In continents like Africa the development of FPLLI poses a tantalizing and insurmountable problem as one person can receive as many as eighteen *P. falciparum* infectious mosquito bites per day during the high transmission season. The putative vaccine candidate RTS,S/ASO1 provides a clear example [8], since the suggested protective immunity (considering protection to be less than 5000 parasites per microliter of blood) was short-lived (less than 6 months) [8] in only 27% of the vaccinated population after the fourth booster immunization 6 months later [9]. The WHO thus did not recommend its use for infants [9].

For more than three decades we have pursued the idea that fully-protective immunity: zero parasites in the blood or spontaneous rapid and permanent recovery after very low parasitaemia (less than 0.1%) can be induced with chemically-synthesized vaccines, based on the concept that functionality relevant **c**onserved **h**igh **a**ctivity **b**inding **p**eptides (cHABP) have to be recognized in the corresponding [10] protein to properly modify them (mHABP) and render them highly immunogenic and protection-inducing [11]. Such minimal subunit-based mHABPs must fulfil set physicochemical and topochemical rules (previously described) to properly display a perfect fitting into MHCII-pep-TCR complex [12].

That goal was achieved when a large number of highly **i**mmunogenic **p**rotection-**i**nducing **p**eptide **s**tructures (IMPIPS) [13] fulfilled those requirements when used as individual epitopes in primary challenges.

Therefore these merozoite-derived IMPIPS which had demonstrated clear FPLLI against experimental challenge with the highly-infectious *Aotus* monkey-adapted *P. falciparum* FVO strain were used to solve the immunological memory problem. **Protected** monkeys and some **non-protected** ones kept in captivity after challenge, after all of them had received anti-malarial treatment (to clear any residual parasites), were then **re-challenged** 60 days later (after all traces of anti-malarial drugs had disappeared) to determine the development of FPLLI. By the same token, sera from *Aotus* monkeys immunized with Spz-derived IMPIPS and kept in captivity for up to 900 days (~2 ½ years) after the first immunization were analysed for the presence of **v**ery **h**igh **l**ong-**l**asting **a**ntibody (VHLLA) titres against *P. falciparum* Spz, as determined by immunofluorescence assay

* Corresponding author. Fundación Instituto de Inmunología de Colombia (FIDIC), Bogotá D. C., Colombia.
Email address: mepatarr@gmail.com (M.E. Patarroyo)

http://dx.doi.org/10.1016/j.bbrc.2016.06.115
0006-291/

(IFA), and their corresponding recombinant proteins by western blot (WB), to determine antibody titre duration [14].

2. Materials and methods

2.1. IMPIPS

mHABPs were synthesized according to Merrifield's peptide synthesis methodology, as modified by Houghten and thoroughly described [10]; a 600 MHz spectrometer was used for determining the ^{1}H NMR 3D structure of a large panel of mHABPs [11].

2.2. Monkeys

Wild-caught *Aotus* monkeys from the Amazon jungle were used for trials authorized by Colombian environmental authorities (CORPOAMAZONIA, permission number 0632 and 0042/2010); they were kept in our field-station in Leticia (Amazon department capital), looked after by expert veterinarians and workers supervised weekly by expert biologists and veterinarians from the local environmental authorities and ethics committee. After the study was completed they were treated with paediatric doses of chloroquine, kept in quarantine for 20 more days and released back into the jungle close to their capture site, accompanied by environmental authority officials. Those participating in this trial were kept according to methods above described.

2.3. Immunization

After arriving at our field station, monkeys were de-parasitized, kept in quarantine for twenty days and fed on a hypercaloric, hyperproteic diet before experiments commenced. Each monkey received 150 μg polymerized IMPIPS subcutaneously, in complete Freund's adjuvant, on day zero; a second dose of the same IMPIPS with incomplete Freund's adjuvant was administered 20 days later. They were challenged 20 days later.

2.4. First challenge

This involved intravenous inoculating 100,000 erythrocytes infected with the highly-virulent *Aotus*-adapted *P. falciparum* FVO strain freshly obtained from another infected *Aotus* monkey [11]; intravenous challenge with a 100% infectious, virulent *P. falciparum* malaria strain being the most stringent vaccine testing methodology.

2.5. Assessing infection

Parasitaemia was determined by fluorescence microscopy using Acridine Orange staining; the percentage of parasitized RBC in their blood was counted, starting on day five. Protected monkeys in their first or primary challenge had no parasites in their blood while **non-protected ones started showing parasites** by day five, reaching ≥6% parasitaemia on days eight to ten; they were immediately treated with paediatric doses of chloroquine. All protected and **non-protected** monkeys were treated after the experiment ended (day 20 after challenge) and kept in quarantine.

2.6. Determining antibodies

IFA titres were determined as previously described [11], blood samples being taken one day prior to the first immunization (i.e. pre-immune - PI) or ten days after the second dose (II_{10}) and 20 days after the second immunization (II_{20}), the day before challenge.

Total schizont lysate or recombinant proteins containing the aa sequence from which the IMPIPS were derived were used for WB.

2.7. Re-challenge

No further immunizations were performed after the second dose was given at the beginning of the experiment. All protected and some **non-protected** monkeys were kept in quarantine for a further 60 days and **re-challenge** with 100,000 iRBC freshly-obtained from another previously-infected monkeys parasitaemia was assessed as before. Two trials (A and B) were performed with two different groups of IMPIPS used for immunization in the first challenge.

2.8. HLA-DRβ binding IMPIPS*

The NetMHCIIpan-3.0 algorithm (predictor of peptide binding to MHC-II molecules), having >95% specificity and 90% sensitivity accurately, predicting (≥90%) correct HLA-DR peptide binding cores (previously determined by X-ray crystallography) was used. This *in silico* method identifies peptides having very high theoretical binding to specific HLA-DRβ1* alleles and alternative β-chain isotypes like HLA-DRβ3*, β4* and β5* alleles measured as peptides half **i**nhibitory **c**apacity (IC ≤ 100 nM), based on the Immune Epitope Database [15].

2.9. Determining 3D structure

600 MHz spectrometer ^{1}H NMR 3D structures were determined with RP-HPLC-purified IMIPS; their sequential connectivities and dihedral angles have already been described [13,14,16–19]. Only χ1 angle degrees of residues considered TCR contacting (positions p2, p5, p8) regarding their binding in the HLA-DR peptide binding region (PBR) are described, based on their predicted binding to HLA-DR molecules. For other very relevant TCR contacting residues (p3, p7) their rotameric orientation and relevant immunological functions have been already described [14].

3. Results and discussion

Reminder: All participating monkeys were immunized only twice with a single IMPIPS; immune protection was therefore elicited by just two doses of individual IMPIPS.

3.1. Antibodies

Remarkably, Group I (protected) and Group II (non-protected) antibody (Ab) patterns, titres and reactivities (assessed by IFA and WB) were extremely similar prior to the first-**challenge** (Table 1), as can be appreciated when comparing cHABP 4044-derived MSP-2 **24112** (protected) and **22774** (non-protected) analogue mHABPs (Table 1) as assessed by IFA and WB (Fig. 1B, *Aotus* 16087 and 12877 respectively). Similarly the Ab reactivity by IFA of SERA-5 6725-derived **22830** (protected) and **24216** (non-protected) derived from 6746 were very similar by WB analysis (not shown).

It is thus extremely difficult to distinguish between permanent long-lasting protective epitopes and permanent short-protective ones based on actual Ab reactivity; such thoroughly-described phenomenon shows the exquisite reactivity of the immune response regarding FPLLI induction.

Table 1
IMPIPS molecule of origin and our laboratory's serial number in bold; below the native cHABP number, aa sequence; distance between the farthest atoms in pockets 1 and 9, measured in Å; (NA = not-applicable), antibody titres as assessed by IFA, the prefix the number of monkeys displaying such titre, PI = pre-immune 20 days after the second dose and performance after first challenge including the number of fully protected monkeys and those protected after **re-challenge** (+o −). Colours indicate residues fitting into HLA-DRβ1* PBR pockets: fuchsia pocket 1, blue pocket 4, orange pocket 6 and green pocket 9. TCR-contacting residues in this study (p2, p5, p8) are indicated.

PROTEIN PEPTIDE		SEQUENCE	P1-P9 Distance (Å)	IFA TITERS PI	IFA TITERS II20	Protection First Challenge	Protection RE Challenge
		GROUP I					
		P1 p2 p5 p8 P9					
MSP-2	**24112** 4044	S K Y S N T F N I N A **Y N M V I R R S M**	26.5	0	1(1280)	II/8	+
AMA-1	**22780** 4313	G E D A E V A G T Q Y **F H P S G K V P V** F G	26.6	0	1(1280)	II/10	+
MSP-1	**22770** 1585	**Y H L P L G G V Y** R A L K K Q	26.6	0	2(640)	II/9	+
EBA-175	**22814** 1783	N D K L **Y R M E Y W K T I** K K D V W	25.9	0	2(5120)	I/10	+
SERA-5	**22830** 6725	L K M T N N A I S F **M S P S S S L E K** K	26.5	0	1(160)	I/10	+
SERA-5	**22834** 6737	D H I H V K M F **K V I E N N D K** S E L I	25.6	0	1(2560)	II/9	+
CSP-1	**25608** 4383	K N S **F S L G E N P N A** N P	27.5	0	2(2560)	ND	ND
CSP-1	**32958** 4388	G N G Q G **L N M N N P P N F** N V D E N A	27.1	0	3(1280)	ND	ND
STARP	**24320** 20546	V I K H M R **F H A D Y Q A P F** L G G G Y	NA	0	1(320)	ND	ND
		GROUP II					
		P1 p2 p5 p8 P9					
MSP-2	**22774** 4044	K N E S K Y S N T **F E V N A Y N M V** N R	22.3	0	1(2560)	II/10	-
MSP-1	**24148** 5501	M L N **I S M L Q T V M M** M T P Q K	19.0	0	1(2560)	II/8	-
EBA-175	**22812** 1779	N N D R I **Y D M N H L M I K** M H I L A I	21.5	0	1(2560)	I/9	-
EBA-175	**24166** 1818	F N N I P S R **Y N L Y D K M L P** L D D	21.7	0	1(160)	II/5	-
EBA-175	**24150** 1758	W K S Y S **V D D N I P M N M** S L I H K H	21.2	0	1(1280)	II/7	-
HRP-II	**24230** 6800	S A F D D N **L T A A N A M G L** I L N K R	21.6	0	2(320)	II/7	-
SERA-5	**24216** 6746	D Q G N T **I T A W N R A A K** F H L E T I	22.3	0	2(640)	II/8	-
TRAP	**24246** 3289	S P T S **V T V G K G A F S** F K A E	21.0	0	1(1280)	ND	ND
SPECT-2	**38890** 34938	S D **Y T K A L A A E A** K V S G S Y W G I	18.6	0	1(640)	ND	ND

Furthermore, IFA, ELISA or WB serological analysis involving recombinants fragments prior to high malarial transmission seasons have shown that the bulk of immune response is directed against highly polymorphic, hypervariable regions of the molecule, the same occurs when immunizing humans or experimental animals with X-ray attenuated whole Spz, recombinant proteins, DNA vector based fragments, etc., showing that polymorphism is a very common mechanism used by microbes to escape immune pressure. Such approach (immunological) to epitope selection has been exhaustively shown to be inappropriate in countless human vaccine trials [20] due to skewing the immune response towards highly polymorphic hypervariable regions.

3.2. Immunogenetic analysis

Genetic restriction ascribed to a particular HLA-DRβ1* allele represents an alternative to such long-lasting protective response but it is extremely difficult to ascertain due to the tremendous polymorphism this region displays. The NetMHCIIpan-3.0 algorithm revealed no preference for any HLA-DRβ1* allele, since the same alleles were present in both groups (I and II) but showing a skewing towards binding to alternative β-chain HLA-DRβ3*, β4* and β5* alleles in the **non-protected** group II (Table 2). Such preference deserves further analysis.

3.3. Protection against re-challenge

Two trials (A and B) performed with different Mrz-derived IMPIPS to cover the MHC-II genetic restriction, trying to address memory or FPLLI phenomena, produced similar results (Fig. 2) when these previously protected monkeys were **re-challenge**.

Three IMPIPS-induced FPLLI: 1585 MSP-1-derived **22770** (*Aotus* 12824), 6737 SERA-5-derived **22834** (*Aotus* 12984) and 4044 MSP-2-derived **24112** (*Aotus* 16006 and 16087) in some immunized monkeys having complete absence of parasites in their blood during the whole trial All these IMPIPS showed high binding capacity to HLA-DRβ1* alleles but none bound to HLA-DRβ3*, β4* or β5* alleles.

Short-lived (~5 days), very low parasitaemia (<0.1%) that spontaneously recovered, not showing any more parasites during the rest of the experiment was seen in some previously-protected monkeys participating in **re-challenge** trial involving other IMPIPS (cHABP 4313 AMA-1-derived **22780**, cHABP 6725 SERA-5-derived **22830**, and cHABP 1783 EBA-175-derived **22814**). Therefore they were considered protective IMPIPS since parasitaemia was very low and rapidly cleared being this behaviour totally different to the well-known semi-immune chronicity phenomena. The latter two IMPIPS: **22830** and **22814** bound with high capacity to HLA-DRβ1* molecules and simultaneously to HLA-DRβ5*0101/0102 and HLA-DRβ5*0202 alleles (Table 2).

Another striking finding that correlates with the previous observation is that all **non-protection** inducing in **re-challenge** IMPIPS

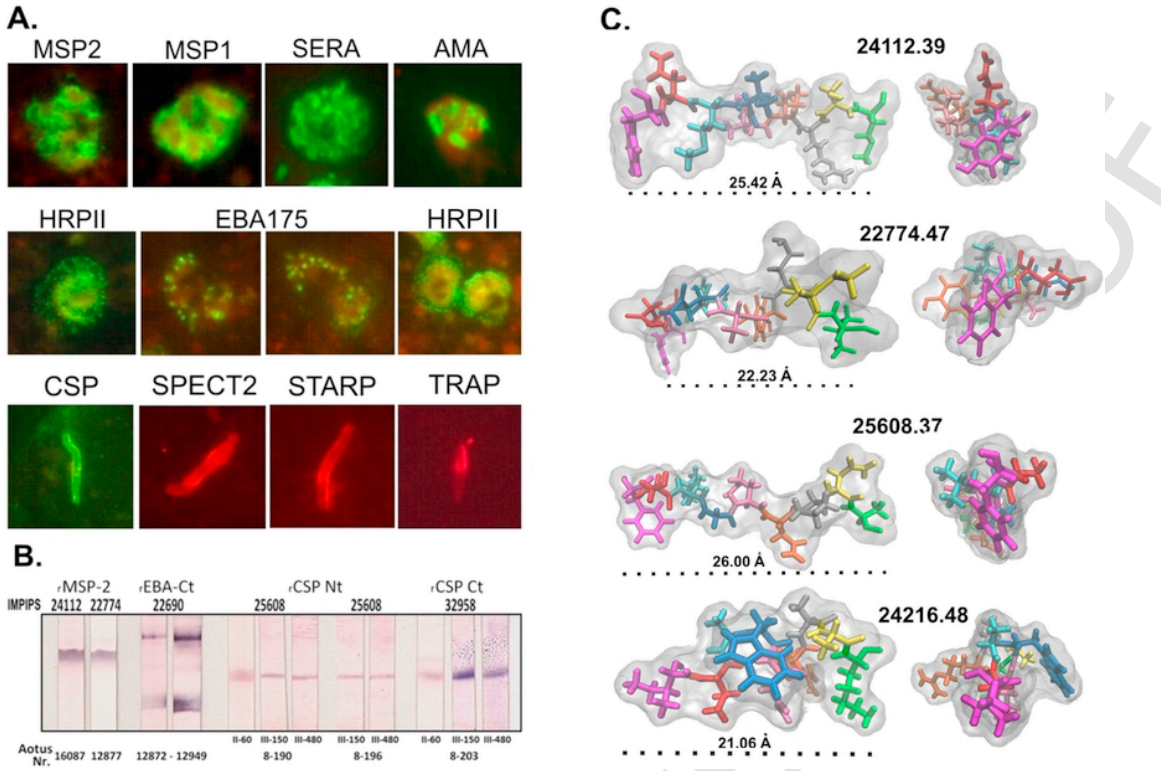

Fig. 1. A. Immunofluorescence patterns recognized by sera from *Aotus* monkeys immunized with specific IMPIPS and determined by immunofluorescence. MSP-2 and MSP-1 detected on the **m**embrane **s**urface **p**roteins; SERA-5, **s**erine **r**epeat **a**ntigen-5 intracytoplasmic; AMA-1, **a**pical **m**erozoite **a**ntigen: present on the apical and Mrz membrane; HRP-II histidine-rich protein II: identified as small intra-erythrocyte dots; EBA-175, **e**rythrocyte **b**inding **a**ntigen-175 present in micronemes. CSP-1 membranal **c**ircumsporozoite **p**rotein-**1**; SPECT-1 **s**porozoite **m**icroneme **p**rotein **e**ssential for **c**ell **t**raversal-1 identified in membrane and micronemal small dots; STARP **s**porozoite **t**hreonine and **a**sparagine-**r**ich protein, and TRAP **t**hrombospondin-**r**elated **a**nonymous **p**rotein, identified in rhoptries and micronemes. **B**. WB analysis of MSP-2 (4044) **24112** immunized and **re-challenge** protected monkeys compared to (4044) **22774** MSP-2 immunized **re-challenge** and **non-protected** monkey. **C**. IMPIPS lowest energy conformer 3D structure determined by 600 MHz ^{1}H NMR identified by our serial number followed by dot corresponding to conformer number. Amino-acid colour based on HLA-DRβ1* binding activities, binding motifs, and binding registers as follows: pocket 1, fuchsia; p2, red; p3, turquoise; pocket 4, dark blue; p5, rose; pocket 6, light brown; p7, gray; p8, yellow and pocket 9, green. The distances between the farthest atoms of residues fitting into pockets 1 and 9 are measured in angstroms (Å). (For interpretation of the references to colour in this figure legend, the reader is referred to the web version of this article.)

(group II) display shorter (22.5 Å ± 1.5 Å) structures (Table 1) as determined by ^{1}H NMR (Fig. 1C. IMPIPS **22774.47** and **24216.48**, for example) when compared with all group I IMPIPS having 26.5 Å ± 1.5 Å (Table 1) distances between residues fitting into HLA-DRβ1* PBR pockets 1 to 9 (Fig. 1C. IMPIPS **24112.39** and **25608.37**, for example). Group I IMPIPS totally displayed complete polyproline type II left-handed ($PPII_L$) structures while group B displayed a mixture of α-helical and $PPII_L$ structures, making them ±3.0 Å shorter. Such clear and neat difference had not been observed previously, due to the fact that **re-challenge** experiments had not been performed beforehand; therefore, our previously reported distances for IMPIPS were 26.5 Å ± 3.5 Å which included both groups (I and II).

Most monkeys which were **not protected** in **re-challenge** trials displayed greater binding capacity to HLA-DRβ3*, β4* or β5* alleles (Table 2), suggesting these IMPIPS clear skewing regarding their binding to these MHC-II alleles. It might be speculated that such preferential HLA-DRβ3*, β4* or β5* binding could bias the immune response towards short-lived memory protective immunity. Supporting such information, we have previously shown that peptides inducing short-lived antibody responses against *P. falciparum* malaria have shorter structure registers between aa fitting into the HLA-DRβ1* peptide binding region (PBR) as determined by ^{1}H NMR spectrometry and are read in a different MHC-II functional register [21].

X-ray crystallography has shown that HLA-DRβ3* molecules are 2.0 Å wider in Kβ71 than DRβ1*, that Wβ61 is rotated 90° and more distant from pocket 9, that α76R is notably displaced upwards leaving pocket 9 highly hydrophobic, that H-bonds between peptide backbone atoms and DRβ3* interacting residues are >4 Å distant, making these interaction between DRβ3*-IMPIPS longer, unstable and weaker for stimulating an appropriate immune response. All of these stereo chemical characteristics could probably be associated with short memory induction [22,23].

Since IMPIPS cannot be involved in Spz challenge, due to irreproducible results regarding the only *Anopheles* mosquito-derived *P. falciparum* strain (Santa Lucia) adapted to *Aotus* monkeys, such antibodies' permanence in Spz-derived IMPIPS immunized monkey sera was determined by IFA and WB with recombinant fragments corresponding to the protein from which the aa sequence was derived. Monkeys, kept in our field station in the Amazon jungle for 900 days after the 1st vaccination, followed-up for 840 days after the 3rd dose (~2½ years) with IMPIPS CSP-1 4383-derived **25608**; 4389-derived **32958** and STARP **24230** 20546-derived produced very high and long-lasting Ab titres (Fig. 1B). Some others like 3289-derived TRAP **24246** and SPECT-2 34938 derived **38890** had high Ab titres that slowly declined over a 6-month period. This last **v**ery-**h**igh, **l**ong-**l**asting **a**ntibody-**i**nducing (VHLLAI) mHABP also had high binding to HLA-DRβ5*0202 allele molecules.

Table 2
IMPIPS inducing merozoite-FPLLI or sporozoite-VHLLAI. HLA-DRβ1* or β3*, β4*, β5* alleles binding activity and their IC below in parenthesis based on the NetMHCIIpan-3.0 method. According to their PBR register, TCR-contacting residues p2, p5, p8 side-chain χ1 angles are described.

		HLA-DRβ1*	HLA-DRβ3*,β5*	p2	p5	p8
				χ1	χ1	χ1
GROUP I						
MSP-2	24112.39	0101/0102 25.6-30.0	--	-83.7	+68.1	+66.5
AMA-1	22780.43	0101/0102/1303/1305 94.0-123.0-128.0-111.0	--	-170	Gly	Pro
MSP-1	22770.15	1330/1303/1425/1201 20.7-67.5-61.7-24.6	--	-173	+65	+89.9
EBA-175	22814.42	1303/1330 67.6-20.7	β5*0101/0102 29.0-29.6	-71	-146	+56.4
SERA-5	22830.20	0901/0902 76.5-53.5	β5*0202 23.6	-169	-174	+66.0
SERA-5	22834.42	0102 50.9	--	+64	-60.1	+56.9
CSP-1	25608.37	0101 278.6	--	-174	-58	+80.0
CSP-1	32958.2	1303 132.9	--	-77.7	-171.9	+8.1
STARP	24320.18	1303/1330 168.4-107.6	β3*0101/0201 56.2-170.1	-113	-166	+19.3
GROUP II						
MSP-2	22774.36	0101/0102 122.0-124.0	β5*0202 111,6	-173	Ala	-167.1
EBA-175	22812.20	1102/1301 94.2-94.2	β3*0201/0301 48.1-32.3	-168	-167	-68,9
MSP-1	24148.7	0101/0102/1201 17.7-57.0-8.2	β3*0301/β4*0401/β5*0202 67.4-75.8-93.0	+63.0	-94.3	-72.1
EBA-175	24166.13	1201/1330/1406 119.0-102.0-110.0	β5*0101/0102 29.0-74.0	-168	-59.3	-58.6
EBA-175	24150.47	0301 230.4	β3*0101 100.7	-170	-61	-62
HRPII	24230.13	0701/0101/0102 92.3-24.9-14.5	β5*0202 30.5	+18.5	+103	Gly
SERA-5	24216.48	1104/1106/0804 13.0-14.2-34.0	β4*0101 331.0	+55	-164	Ala
TRAP	24246.41	0102/0101 70.5-142.9	β5*0202 78.5	+178	+161	Ala
SPECT-2	38890.32	0901/0902/0101/0102 33.7-32.8-8.9-10.9	β5*0101/0102 88.1-68.0	-152	-68	-69.9

3.4. p2 volume in long-lasting protective immunity

Besides the distance between P1 and P9 residues, and φ and ψ angles having $PPII_L$ conformation, we have found volume and charge to be critical physicochemical characteristics for a proper fit into the HLA-DRβ1* PBR. Something similar occurs with upwardly-orientated TCR-contacting residues, as previously shown for p3 and p7 [14]. Table 1 in the present manuscript clearly shows that most FPLLI- and VHLLAI-inducing IMPIPS in group I had a larger volume in p2 than those in groups II, whereas positively-charged residues having π electrons (H, R, K) predominated in group I. Smaller polar residues predominating in group II had alcohol groups (S, T) in their side chains acting as nucleophiles or acidic negatively-charged aa (E, D).

3.5. p8 residue orientation determines long-lasting protective immunity

Protein and peptide studies have thoroughly demonstrated that aa side-chain orientation has tri-modal distribution based on χ1 angle rotation related to a protein or peptide's frontal plane; *gauche*$^+$ (trans to the carbonyl group), *gauche*$^-$ (trans to the Hα atom) or trans (trans to the amino group), except for Gly, Ala and Pro, the later (**warning**) an iminoacid having different χ1 angle rotation, depending on the preceding's residue φ angle. According to χ1 angle rotation degree, aa have been divided into *gauche*$^+$ (−120° to 0°), *gauche*$^-$ (0° to +120°) and trans (trans +120° to +240°). Therefore when the 600 MHz 3D structures of our IMPIPS used for immunization were determined it was found that, strikingly, **all protected** *Aotus* monkeys during **re-challenge** had been vaccinated with IMPIPS having χ1 angles ranging from +89.9° to +8.1° in residues located in p8 (Table 2), therefore having *gauche*$^-$ aa side-chain orientation in p8. By contrast, all **non-protected** monkeys in **re-challenge** had been immunized with IMPIPS having −167.1° to −12.3° rotation angles, therefore *gauche*$^+$ orientation in p8 (Table 2).

VHLLAI Spz-derived IMPIPS (**25608**, **32958** and **24320**) and Mrz-derived FPLLI **24112** included in mixtures [14] not blocking, interfering or suppressing each other's activity had also *gauche*$^-$ side-chain orientation in p8.

When analysing the aa sequence of IMPIPS used to immunise **re-challenge** protected monkeys, p8 was occupied by polar residues (S, T, E, D), the same as those Spz derived VHLLAI IMPIPS (N, N, P), except for AMA-1-derived **22780** and STARP-derived **24320** both having the iminoacid Pro (which could be puckered up or down) and **22770** having Val in this position (Table 1. Group I). Strikingly, all **non-protected** monkeys during **re-challenge** were immunized with IMPIPS having apolar residues in p8 (M, I, M, L, N, G, A, F), except

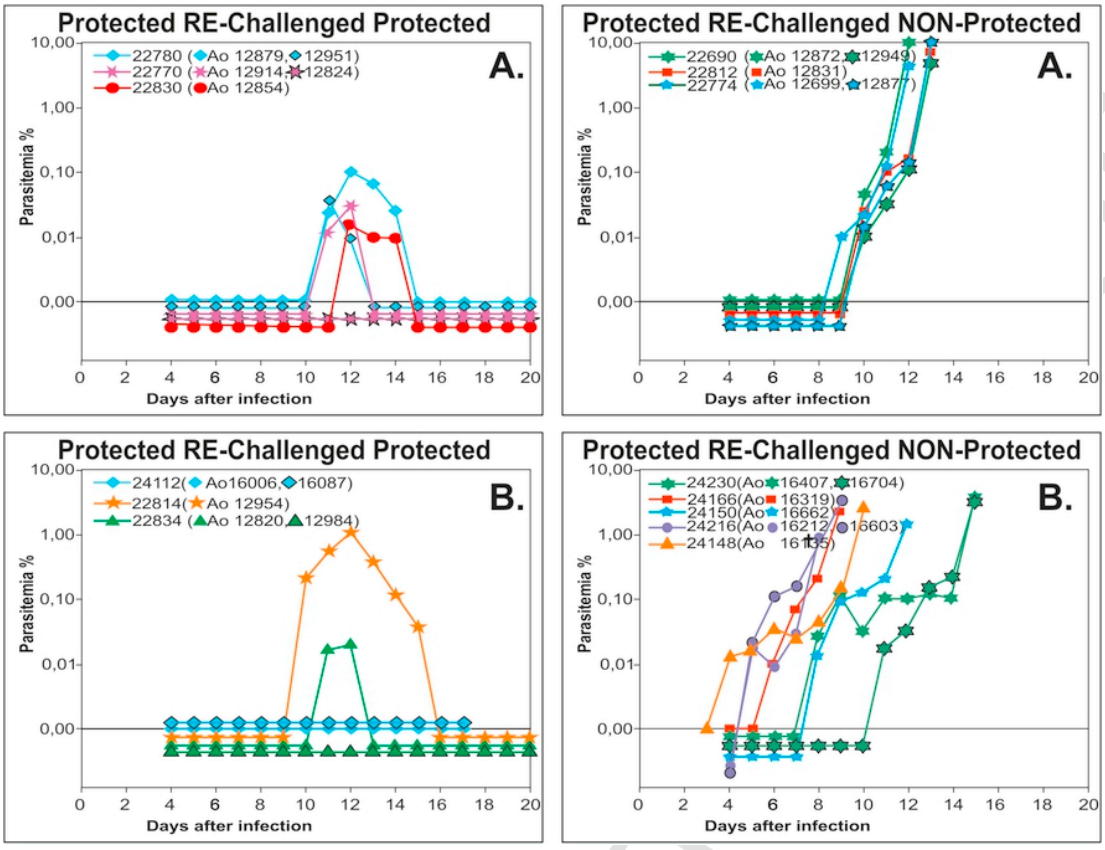

Fig. 2. Parasitaemia levels, percentage of infected RBC (%) displayed in a semi-logarithmic scale as assessed by AO staining in, monkeys participating in **re-challenge** trials A and B group I (protected); group II (non-protected) on days after **re-challenge**.

for **38890** (E) (Table 1) including the Spz derived IMPIPS **24246** and **38890** inducing short lived Abs titres.

Our previous data regarding IMPIPS previously reported 3D structures has shown the critical role of χ1 angle in residues p3 and p7, having *gauche*$^+$ orientation associated with being able to be mixed to induce FPLLI and VHLLAI without interfering, blocking, suppressing, abolishing or poisoning each other's immunological activity in the process of developing a complete multi-epitope, multi-stage minimal subunit-based, chemically-synthesized antimalarial vaccine. Conversely, the completely abolished immune response induced in mixtures with other IMPIPS when mixing them i.e. **24148** and **24246** corresponds to the same IMPIPS which could not induce either **re-challenge** protection or VHLLAI memory; these IMPIPS also displayed *gauche*$^+$ orientation in p8 (Table 2. Group II) suggesting some stereo-chemical interference in memory induction and combination in mixture composition.

In intracellular pathogenic diseases the development of poly-functional, rapidly proliferating T-cells, with low apoptosis seems to be the key issue [24] to clear infection and develop a robust T-cell memory [25] and many hypotheses have arisen for explaining the absence of memory induction, i.e. T-cell exhaustion after infection [26] leading to the loss of parasite-specific memory T-cells inducing protection from re-infection [27], (as in this manuscript), or alternative up-regulation of FOXP3 expressing $CD4^+$ $CD25^+$ T-regulatory cells associated with more rapid parasite growth during infection [28] or elevated number of highly suppressive T-regulatory cells in severe malaria [29].

Alternative explanations are the induction of **p**rograme**d** cell **d**eath-1 (PD-1) molecules on activated $CD4^+$ or $CD8^+$ T-cells that in conjunction with LAG-3+ T-cells modulate immunity against malaria [30]. It has been recently demonstrated in mice having the PD-1 gene deleted (PD-1KO) that such deletion generates sterile protective immunity, unlike wild type mice infected with *Plasmodium chabaudi* which maintained ~1% parasitaemia [31] equivalent to human chronic subclinical malaria.

There are many more alternative hypothesis associated with the lack or absence of protective immunity memory but this 3D structural analysis of 20 IMPIPS clearly suggested that p8 residue χ1 angle rotation and orientation is associated with or determines long-lasting protective memory.

We therefore suggest that in a complete, fully-protective minimal subunit-based, chemically-synthesized vaccine able to induce very **l**ong-**l**asting **p**rotective **i**mmunological memory, besides the previously-described physicochemical principles regarding a perfect fit, into the HLA-DRβ1*PBR, TCR-contacting residues p3 (apolar) and p7 (also apolar) should have *gauche*$^+$ rotamer orientation [14] while p8 (polar) should have *gauche*$^-$ orientation and p2 should have the polar characteristics shown here. These findings allow us to propose that such stereo chemical and topological rules mediate FPLLI memory.

This is the first time protective memory induction has been shown, at 3D structural level to be associated with specific electronic and rotamer orientation of a particular TCR-contacting residue (p8) while negatively associated also with a binding capacity to HLA-DRβ3*, β4* or β5* allelic molecules, paving the way for a logical rational methodology for long-lasting protective immunity.

Conflict of interest

The authors declare that they have no financial or commercial conflicts of interest.

Acknowledgments

This research was supported by "The Colombian Science, Technology and Innovation Department (Colciencias)", Contract RC#0309-201.

We would like to thank Mr. Jason Garry for his collaboration in the translation of this manuscript.

References

[1] S. Dutta, S.Y. Lee, A.H. Batchelor, D.E. Lanar, Structural basis of antigenic escape of a malaria vaccine candidate, Proc. Natl. Acad. Sci. U. S. A. 104 (2007) 12488–12493.

[2] D.P. Eisen, A. Saul, D.J. Fryauff, J.C. Reeder, R.L. Coppel, Alterations in Plasmodium falciparum genotypes during sequential infections suggest the presence of strain specific immunity, Am. J. Trop. Med. Hyg. 67 (2002) 8–16.

[3] W.D. Morgan, M.J. Lock, T.A. Frenkiel, M. Grainger, A.A. Holder, Malaria parasite-inhibitory antibody epitopes on Plasmodium falciparum merozoite surface protein-1(19) mapped by TROSY NMR, Mol. Biochem. Parasitol. 138 (2004) 29–36.

[4] W.D. Morgan, T.A. Frenkiel, M.J. Lock, M. Grainger, A.A. Holder, Precise epitope mapping of malaria parasite inhibitory antibodies by TROSY NMR cross-saturation, Biochemistry 44 (2005) 518–523.

[5] C.Q. Schmidt, A.T. Kennedy, W.H. Tham, More than just immune evasion: hijacking complement by Plasmodium falciparum, Mol. Immunol. 67 (2015) 71–84.

[6] J.Y.A. Doritchamou, VAR2CSA domain-specific analysis of naturally acquired functional antibodies to P. falciparum placental malaria, J. Infect. Dis. (2016).

[7] F. Farooq, E.S. Bergmann-Leitner, Immune escape mechanisms are Plasmodium's secret weapons foiling the success of potent and persistently efficacious malaria vaccines, Clin. Immunol. 161 (2015) 136–143.

[8] Efficacy and safety of RTS, S/AS01 malaria vaccine with or without a booster dose in infants and children in Africa: final results of a phase 3, individually randomised, controlled trial, Lancet 386 (2015) 31–45.

[9] W.H.O. (WHO), Malaria vaccine, Wkly. Epidemic 9 (2016) 33–52.

[10] L.E. Rodriguez, H. Curtidor, M. Urquiza, G. Cifuentes, C. Reyes, M.E. Patarroyo, Intimate molecular interactions of P. falciparum merozoite proteins involved in invasion of red blood cells and their implications for vaccine design, Chem. Rev. 108 (2008) 3656–3705.

[11] M.E. Patarroyo, A. Bermudez, M.A. Patarroyo, Structural and immunological principles leading to chemically synthesized, multiantigenic, multistage, minimal subunit-based vaccine development, Chem. Rev. 111 (2011) 3459–3507.

[12] M.A. Patarroyo, A. Bermudez, C. Lopez, G. Yepes, M.E. Patarroyo, 3D analysis of the TCR/pMHCII complex formation in monkeys vaccinated with the first peptide inducing sterilizing immunity against human malaria, PLoS One 5 (2010) e9771.

[13] M.E. Patarroyo, A. Bermudez, M.P. Alba, M. Vanegas, A. Moreno-Vranich, L.A. Poloche, M.A. Patarroyo, IMPIPS: the immune protection-inducing protein structure concept in the search for steric-electron and topochemical principles for complete fully-protective chemically synthesised vaccine development, PLoS One 10 (2015) e0123249.

[14] A. Bermudez, D. Calderon, A. Moreno-Vranich, H. Almonacid, M.A. Patarroyo, A. Poloche, M.E. Patarroyo, Gauche(+) side-chain orientation as a key factor in the search for an immunogenic peptide mixture leading to a complete fully protective vaccine, Vaccine 32 (2014) 2117–2126.

[15] M. Andreatta, E. Karosiene, M. Rasmussen, A. Stryhn, S. Buus, M. Nielsen, Accurate pan-specific prediction of peptide-MHC class II binding affinity with improved binding core identification, Immunogenetics 67 (2015) 641–650.

[16] M.E. Patarroyo, A. Moreno-Vranich, A. Bermudez, Phi (Phi) and psi (Psi) angles involved in malarial peptide bonds determine sterile protective immunity, Biochem. Biophys. Res. Commun. 429 (2012) 75–80.

[17] M.E. Patarroyo, A. Bermudez, M.P. Alba, The high immunogenicity induced by modified sporozoites' malarial peptides depends on their phi (varphi) and psi (psi) angles, Biochem. Biophys. Res. Commun. 429 (2012) 81–86.

[18] M.E. Patarroyo, M.A. Patarroyo, L. Pabon, H. Curtidor, L.A. Poloche, Immune protection-inducing protein structures (IMPIPS) against malaria: the weapons needed for beating Odysseus, Vaccine 33 (2015) 7525–7537.

[19] M.E. Patarroyo, G. Arevalo-Pinzon, C. Reyes, A. Moreno-Vranich, M.A. Patarroyo, Malaria parasite survival depends on conserved binding peptides' critical biological functions, Curr. Issues Mol. Biol. 18 (2015) 57–78.

[20] S. Li, M. Plebanski, P. Smooker, E.J. Gowans, Editorial: why vaccines to HIV, HCV, and malaria have So far failed-challenges to developing vaccines against immunoregulating pathogens, Front. Microbiol. 6 (2015) 1318.

[21] M.E. Patarroyo, M.P. Alba, L.E. Vargas, Y. Silva, J. Rosas, R. Rodriguez, Peptides inducing short-lived antibody responses against Plasmodium falciparum malaria have shorter structures and are read in a different MHC II functional register, Biochemistry 44 (2005) 6745–6754.

[22] C.S. Parry, J. Gorski, L.J. Stern, Crystallographic structure of the human leukocyte antigen DRA, DRB3*0101: models of a directional alloimmune response and autoimmunity, J. Mol. Biol. 371 (2007) 435–446.

[23] S. Dai, F. Crawford, P. Marrack, J.W. Kappler, The structure of HLA-DR52c: comparison to other HLA-DRB3 alleles, Proc. Natl. Acad. Sci. U. S. A. 105 (2008) 11893–11897.

[24] J.R. Lukens, M.W. Cruise, M.G. Lassen, Y.S. Hahn, Blockade of PD-1/B7-H1 interaction restores effector CD8+ T cell responses in a hepatitis C virus core murine model, J. Immunol. 180 (2008) 4875–4884.

[25] E.J. Wherry, T cell exhaustion, Nat. Immunol. 12 (2011) 492–499.

[26] M.N. Wykes, J.M. Horne-Debets, C.Y. Leow, D.S. Karunarathne, Malaria drives T cells to exhaustion, Front. Microbiol. 5 (2014) 249.

[27] R. Stephens, J. Langhorne, Effector memory Th1 CD4 T cells are maintained in a mouse model of chronic malaria, PLoS Pathog. 6 (2010) e1001208.

[28] M. Walther, J.E. Tongren, L. Andrews, D. Korbel, E. King, H. Fletcher, R.F. Andersen, P. Bejon, F. Thompson, S.J. Dunachie, F. Edele, J.B. de Souza, R.E. Sinden, S.C. Gilbert, E.M. Riley, A.V. Hill, Upregulation of TGF-beta, FOXP3, and CD4+CD25+ regulatory T cells correlates with more rapid parasite growth in human malaria infection, Immunity 23 (2005) 287–296.

[29] G. Minigo, T. Woodberry, K.A. Piera, E. Salwati, E. Tjitra, E. Kenangalem, R.N. Price, C.R. Engwerda, N.M. Anstey, M. Plebanski, Parasite-dependent expansion of TNF receptor II-positive regulatory T cells with enhanced suppressive activity in adults with severe malaria, PLoS Pathog. 5 (2009) e1000402.

[30] N.S. Butler, J. Moebius, L.L. Pewe, B. Traore, O.K. Doumbo, L.T. Tygrett, T.J. Waldschmidt, P.D. Crompton, J.T. Harty, Therapeutic blockade of PD-L1 and LAG-3 rapidly clears established blood-stage Plasmodium infection, Nat. Immunol. 13 (2012) 188–195.

[31] J.M. Horne-Debets, D.S. Karunarathne, R.J. Faleiro, C.M. Poh, L. Renia, M.N. Wykes, Mice lacking Programmed cell death-1 show a role for CD8(+) T cells in long-term immunity against blood-stage malaria, Sci. Rep. 6 (2016) 26210.